Effects of nonequilibrium phonons on the energy relaxation and recombination lifetime of photogenerated carriers in undoped GaAs quantum wells

Kai Shum, M. R. Junnarkar, H. S. Chao, and R. R. Alfano
Institute for Ultrafast Spectroscopy and Lasers, Department of Electrical Engineering and Department of Physics, The City College of New York, New York, New York 10031

H. Morkoç
Coordinated Science Laboratory, College of Engineering, University of Illinois at Urbana-Champaign, Urbana, Illinois 61801-3082

(Received 15 June 1987; revised manuscript received 25 January 1988)

Time-resolved and time-integrated photoluminescence studies of an undoped multiple GaAs quantum-well structure excited by 0.5-ps laser pulses have revealed several important experimental observations on the behavior of photoexcited carriers. A large population of nonequilibrium longitudinal optical phonons produced in the energy relaxation process of hot carriers manifests itself by the nonequilibrium phonon-stimulated phonon replica which is located at ~ 30 meV below $n=1$ electron-hole transition. The energy relaxation is substantially suppressed due to the existence of nonequilibrium phonons after an initial rapid cooling (0–5 ps). The number of photoexcited carriers decreases anomalously fast within the first 30 ps after the excitation by laser pulse. An effective carrier depletion time is determined to be as short as 10 ps. A mechanism which leads to such a short carrier depletion time is associated with the nonequilibrium phonon-stimulated phonon replica.

I. INTRODUCTION

Recently, there has been growing interest in studying the dynamics of photogenerated carriers in semiconductor quantum-well structures since it reflects the fundamental interactions among electrons, holes, and phonons. These interactions determine the performance of ultrahigh-speed electronic and optoelectronic devices. In the case of bulk semiconductors, the slowing of hot-carrier relaxation is attributed to either screening[1] of electron-phonon interactions or reheating of carriers by nonequilibrium (NE) phonons produced in the relaxation process of hot carriers.[2,3] A comparative study[4] of the hot-electron cooling rates in undoped multiple-quantum-well (MQW) structures and in bulk GaAs by time-resolved measurements of optical absorption and gain concluded that the rates were approximately the same at a photogenerated carrier density of 2.5×10^{17} cm^{-3}. This is expected from a simple theory[5] in which lattice is treated as a heat bath for quasiequilibrium carriers. In the case of modulation-doped MQW structures, quasi-steady-state experiments have been carried out from two groups[6,7] to investigate the interaction of electrons and holes with phonons. These experiments have generated conflicting results regarding the presence[6] or absence[7] of NE phonons. Time-resolved PL measurements with ~ 20 ps time resolution were reported by Ryan *et al.*,[8] who found that the cooling of hot carriers was anomalously slow after 40 ps.

Reviewing the aforementioned previous works two important points were noticed. First, one cannot extract information on the initial carrier-relaxation process either from quasi-steady-state experiments or from time-resolved measurements with time resolution greater than 10 ps. To assess the importance of the NE phonon effect on the energy relaxation of hot carriers, one uses a corresponding theory to match the experimental carrier-temperature cooling curve or the logarithm of power loss as a function of the inverse of the carrier temperature. There has been no report on *direct* evidence for the existence of NE phonons in quantum-well structures under high photoexcitation. It is necessary to study the initial carrier-relaxation process to substantiate the existence of NE phonons and its importance on the hot-carrier relaxation since the phonon lifetime is about 7 ps. Second, one cannot easily obtain information on photogenerated carrier lifetime in modulation-doped MQW structures because the large doped-in carrier density is comparable to the photoexcited carrier density. Furthermore, carrier lifetime can influence the cooling of hot carriers.[9] Therefore, it is necessary to study photogenerated carrier dynamics in undoped MQW structures in order to obtain information both on the energy-loss rates and on the carrier lifetime.

In this paper experimental observations are reported from the measurements of time-resolved photoluminescence (PL) with a 2 ps time resolution and time-integrated luminescence spectra from an undoped GaAs MQW structure with dependencies on lattice temperature, excitation intensity, and polarization. The NE phonons emitted by hot electrons are directly observed by measuring the time-integrated as well as time-resolved phonon replica luminescence lying below the $n=1$ electron-to-heavy-hole transition energy. The energy relaxation of hot electrons is found to be substantially suppressed when a large population of NE phonons is

present after an initial rapid cooling. The photoexcited carrier density extracted from a fitting of time-resolved PL profiles at different emitted photon energies decreases nonexponentially and very rapidly within the first 30 ps. An effective carrier-depletion time is determined to be as short as 10 ps. The mechanism leading to such short carrier-depletion time is associated with NE-phonon–stimulated phonon replicas.

II. SAMPLE

The undoped GaAs/$Al_xGa_{1-x}As$ MQW structure investigated was grown by molecular-beam epitaxy on a [001]-oriented undoped GaAs substrate. The MQW consists of 50 periods of 55-Å-thick GaAs and 100-Å-thick $Al_{0.3}Ga_{0.7}As$ layers, and followed by a 1.2-μm-thick GaAs buffer layer. The lateral size of the structure is about 2×4 mm^2. The good quality of the sample is confirmed by well-resolved heavy-hole and light-hole excitonic structures of room-temperature PL spectra. The full width at half maximum (FWHM) for the heavy-hole excitons is about 13 meV. The sample was mounted on the cold finger in an optical helium cryostat.

III. EXPERIMENT

An ultrashort laser pulse of 0.5 ps duration at 620 nm was used to excite the electron-hole pairs in the sample. Most of the light is absorbed in both the GaAs wells and the $Al_xGa_{1-x}As$ barriers. Photogenerated carriers in the barriers will either diffuse to the GaAs buffer layer or be captured into the wells. The latter will result in uncertainty about carrier density in the wells by a fact of ~3. Residual transmitted light is absorbed in the GaAs buffer layer. The diameter of excitation area is about 160 μm. To avoid damaging of the sample surface, the maximum excitation power is adjusted such that photogenerated carrier density is on the order of 10^{19} cm^{-3}. The 0.5-ps laser pulse was generated from a colliding-pulse passive-mode-locked dye laser and amplified by a four-stage dye amplifier pumped with a frequency-doubled Nd:YAG (neodium:yttrium-aluminum-garnet) laser operated at 20 Hz. In order to keep the time resolution of Hamamatsu streak-camera system within 2 ps, PL was spectrally resolved using different narrow-band filters. The luminescence intensities were corrected for the nonlinearity of streak rate, the spectral response, and the transmission of each narrow band. For the time-integrated PL measurements, a Stanford boxcar and a GaAs photomultiplier were used.

IV. RESULTS AND DISCUSSION

A. Steady state

Time-integrated luminescence spectra from the MQW structure excited by the 0.5-ps laser pulse at various lattice temperatures (T_L) are shown in Fig. 1. These spectra were taken in a conventional backward Raman configuration $z(y,y)\bar{z}$, where z is the growth direction. In order to eliminate radiation from the edges of the sample, the luminescence spot was first imaged on an aperture

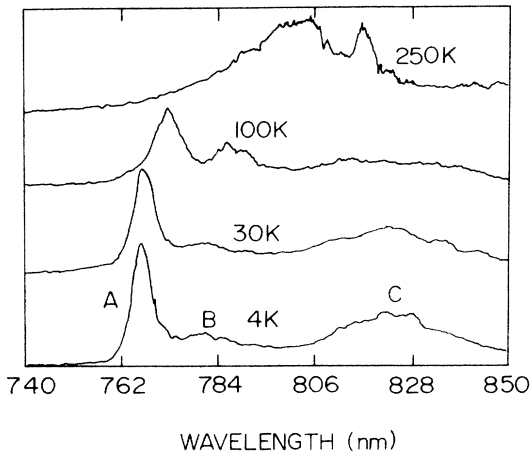

FIG. 1. Time-integrated luminescence spectra at various lattice temperatures. The peaks *A*, *B*, and *C* are explained in the text.

with aid of a streak camera and then refocused onto a vertical slit of a grating spectrometer. Several features are displayed in the data shown in Fig. 1.

(1) The emission band *A* on the high-energy side of the spectra rises from the recombination of photogenerated $n=1$ electrons and heavy holes. The peak of *A* shifts towards the low-energy side as the T_L increases. A high-energy tail on peak *A* develops with increasing T_L.

(2) A broad emission band *C* on the low-energy side of the spectra arises from the GaAs buffer layer. The total emission intensity of *C* decreases as T_L increases.

(3) The most interesting feature of the spectral data is the appearance of an emission band *B*, located about 30 meV below the $n=1$ electron–heavy-hole transition. This *B* emission band is attributed to the NE-phonon–stimulated phonon replica. The following four reasons support this assignment to the *B* band.

(i) This *B* emission band does not appear in the PL spectra taken at low power excitation about 1 W/cm^2 at 4.3 K using the cw 488-nm line of an argon-ion laser. However, the PL spectra using a very weak train of laser pulses (120 fs) directly from the colliding-pulse passive-mode-locked dye laser as the excitation source, with an excitation power density in range of 10^{-5}–10^{-3} W/cm^2, shows a weak electron-to-acceptor emission band separated by 17 meV from the $n=1$ electron–heavy-hole transition accompanied by its phonon replica[10] at low temperatures. This extrinsic emission band disappeared completely when the sample temperature was raised to ~80 K, whereas the *B* band displayed in Fig. 1 exists up to room temperature. Moreover, the relative time-integrated PL intensity of the *B* to *A* band under 0.5-ps light-pulse excitation shown in Fig. 1 decreases as the excitation power density decreases. The *B* band in Fig. 1 is hardly visible when the excitation power density is lower than $10^{-3}P_m$, where $P_m\sim10^{12}$ W/cm^2 is the maximum value of the excitation-power density. This contradicts what is generally expected for impurity emission. Since the concentration of acceptors is low in our sample, as

confirmed by the luminescence studies using the weak train of 120-fs light pulses, an impurity emission band should be more readily apparent and pronounced at lower excitation. Therefore, the B emission band shown in Fig. 1 cannot be attributed to electron-to-acceptor luminescence under high excitation.

(ii) The intensity ratio between the B and A emission bands as indicated by triangles in Fig. 2 increases as lattice temperature increases. To prove the emission band B arises from a NE-phonon–stimulated recombination process, we calculate the sum of occupation numbers both for the equilibrium phonons (lattice temperature T_L) and for the NE phonons (carrier temperature T_c) by assuming that the carrier temperature is the same as the effective temperature for the NE phonons after 30 ps. This will be discussed later with the carrier temperature. The calculated result is shown by the solid line in Fig. 2. The fitting of the total phonon occupation number to the obtained intensity ratio from the spectra is impressively good. This implies that the intensity of band B is well correlated with the LO-phonon population. Because of the participation of the NE phonons the intensity of the B band (also see time-resolved luminescence at 780 nm in Fig. 4) is strongly enhanced, especially at low temperatures. This further supports our assignment of the B band to the NE-phonon–stimulated phonon replica.

(iii) It is also not possible to attribute the emission band B to emission from renormalized band-band transition because the peak position of the A band (766.7 nm) and the B bands at 4.3 K do not change with variation of excitation intensity by a factor of $\sim 10^3$. A further support of the above statement is the fact that the spectral positions of peak A exactly coincide with each other for the two different luminescence studies using different light-excitation sources: one is the weak 120-fs pulse train with a repetition rate of 125 MHz, and the other is the amplified 0.5-ps pulse with a 20-Hz repetition rate.

(iv) We have also studied the polarization of the emission bands A, B, and C by measuring "right-angle"[11,12] $z(y,x)y$ and $z(y,z)y$ integrated luminescence spectra. It was found that the B band emitted at the sample edge along the y direction (see inset of Fig. 3) was highly polarized in the x direction. The A and C emission bands were depolarized, independent of excitation-power density and lattice temperature. The intensity ratio between the x and z directions for the B band is about 20 in the lattice-temperature range from 4.3 to 300 K at full excitation-power density P_m. But the ratio is strongly dependent on the excitation-power density at a given lattice temperature. For example, at $T_L = 20$ K, the ratio decreases from 20 to ~ 6 as the excitation-power density decreases from P_m to $0.017P_m$. Figure 3 shows the spectra for $T = 100$ K at two different excitation intensities. The lower solid trace was taken in the $z(y,x)y$ configuration (TE polarization) at the excitation density of $0.017P_m$. It is identical to the spectrum taken in the $z(y,z)y$ configuration (TM polarization), which is not shown. The B band disappears due to the absence of a large population of NE phonons at the low excitation and high lattice temperature. The upper solid and dashed traces are the TM and TE spectra at the full excitation P_m, respectively. The intensity ratio of TE and TM remains 20. It should be pointed out that the energy position of the A band in Fig. 3 is lower than that in Fig. 1 by ~ 4 meV, while the position of the B band remains unchanged. This low-energy shift of the A band is due to the self-absorption effect. The polarization behavior of the B band is consistent with the results from Raman scattering experiments reported by Zucker *et al.*,[12] where the pump photons are provided by the external laser source. In our case the pump photons arise from the recombination of the $n = 1$ electron and $n = 1$ heavy hole at the subband edges. This process is strongly

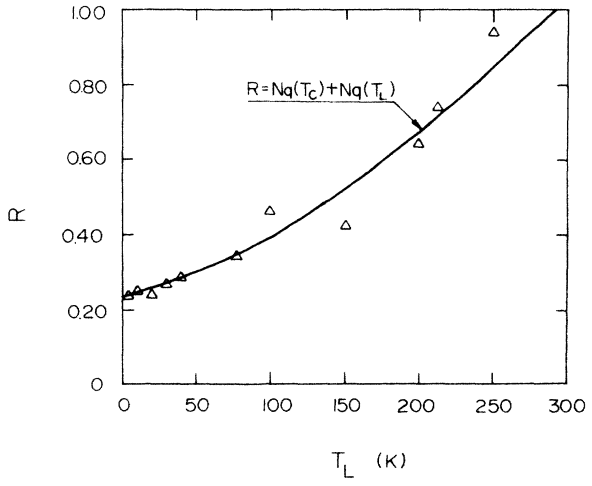

FIG. 2. Triangles are the ratios of the peak intensity of B and A indicated in Fig. 1. The solid curve is explained in the text.

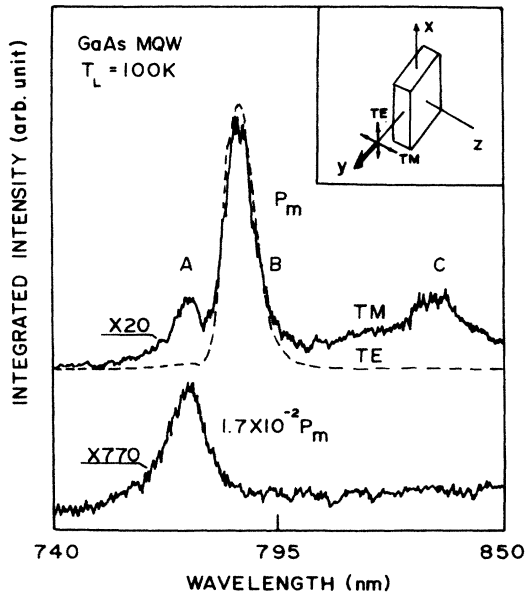

FIG. 3. Time-integrated PL spectra taken in the geometry as shown in the inset at 100 K.

enhanced by the presence of a large number of NE phonons emitted by hot electrons at high excitation. The depolarized feature of band C is expected since the emission is from the GaAs buffer layer. However, the polarization behavior of the emission band A is not understood. In terms of the selection rule of dipole recombination described by Iwamnra *et al.*,[13] the emission intensity of $n=1$ electrons and light holes for the TE polarization should be 4 times larger than that for the TM polarization. There should be no TM emission arising from $n=1$ electron–heavy-hole recombination. It should be mentioned here that the B band in Fig. 1 that was detected along the z direction is depolarized and much weaker, at least by a factor of 20, than detected along the y direction. The former is expected due to the symmetry, and the latter provides an important rule for understanding a fast carrier-density-decreasing process which will be discussed in subsection B.

In order to further substantiate our assignment of the B band, two additional questions must be addressed.

(1) Why no phonon replica appears on the high-energy side of the A band, if a large NE-phonon population really arises? A high-energy replica would arise from a recombination of an energetically elevated electron (hole) by absorbing a phonon and hole (electron). However, the elevated electron (hole) will be very quickly scattered by the other hot electrons (holes) through a strong electron-electron, electron-hole, and hole-hole interaction before it recombines with a hole (an electron). Therefore, the high-energy replica cannot be observed in PL spectra. But this reheating process should result in a retardation of hot-carrier cooling, which is indeed consistent with the time-resolved PL data described in the next section.

(2) Why is the energy separation between the peaks of the A and B bands (E_{AB}), on order of ~ 30 meV, which is smaller than expected (36 meV)? The 30-meV energy separation, in fact, gives a further strong support of our assignment of the B band. In an equilibrium state the interaction strength of an electron and LO phonon in bulk GaAs is proportional to $1/\mathbf{Q}^2$, where $\mathbf{Q}$ is the phonon wave vector. Therefore, the phonons in the vicinity of $\mathbf{Q}=\mathbf{0}$ would be expected to more strongly couple with electrons giving rise to a phonon replica at just 36 meV below its primary emission band. In our highly photoexcited MQW sample, LO phonons are driven to a NE state by a rapid initial-energy-relaxation process of photoexcited hot electrons. The development of these NE states both in the time domain and in two-dimensional wave-vector space ($\mathbf{q}$, parallel to the well plane) has been recently studied by several groups.[14,15] Two important results on the number of NE LO-phonon populations are (i) at given q, it can reach to a maximum in about 0.5–3 ps and then decrease, and (ii) at a given time, it increases steeply from a minimum of $q_{\rm mm}$, reaches to a maximum at q_e, and then decreases. *What is essential concerning the question is that there is a maximum NE LO-phonon population which is located both in a narrow wave-vector space of the vicinity of q_e and in the well plane and lasts in a short time period.* This portion of NE phonons behaves like *coherent bosons*. The existence of the "coherent bosons" will tend to increase the number of the bosons (near q_e) in the system with a rate proportional to the present number of bosons, resulting in a stimulated phonon-emission process. This process can give rise to phonon-replica emissions, when an electron in the conduction subband recombines with a hole in the valence subband—not only a photon, but also a phonon, or more phonons will be emitted to join the boson system. In order to conserve the momentum of an electron-phonon system in this recombination, the electron must possess a momentum of q_e (neglecting the momentum of the emitted photon) which is associated with a kinetic energy of $E_{q_e}=\hbar^2 q_e^2/2m_e$. Therefore, the energy E_{AB} should be equal to LO-phonon energy minus E_{q_e}, which is about 6 meV, corresponding to the values of 1.03×10^6 cm^{-1} and $0.067m_0$ for q_e and electron effective mass m_e. Thus, this gives 30 meV for E_{AB}.

Over years, there has been much debate[13,16–18] over the interpretation of the spectral features located below the $n=1$ electron–to–heavy-hole transition energy, mainly because many species exist in this energy region: LO-phonon replicas, impurity states, and many-body band-gap renormalization. Holonyak and co-workers[17] have demonstrated the LO-phonon participation in GaAs-$Al_xGa_{1-x}As$–based QW laser emission by observing more than one LO-phonon sidebands in the laser operation below the $n=1$ confined-particle transition. Recently, Skolnick *et al.*[18] confirmed that a peak below the $n=1$ electron–heavy-hole transition is a phonon replica by observing the coupling at both the GaAs- and InAs-like bulk LO-phonon energies of a InGaAs QW. Our measurements support these arguments.

B. Time-resolved PL intensities

Time-resolved PL intensities of the MQW structure at 4.3 K were measured over the spectral range from 720 to 780 nm. Four representative streaks at given selected wavelengths are shown in Fig. 4. The emission centered at 770 nm arises from the recombination of band-edge electron and heavy hole. The radiation with wavelengths of less than 770 nm are from the recombination of energetic carriers. The time-resolved luminescence intensity of the phonon replica is centered at 780 nm. Each luminescence profile is an average from 10 individual shots using a prepulse[19] for averaging. The left-hand peak of the dotted curve is the prepulse which reflects the 2-ps temporal resolution. The right-hand peak on the same curve is the Rayleigh-scattering light from the sample surface which defines the "zero" time for our analysis. Several features appear in the data displayed in Fig. 4. (i) The rise time for all the luminescence profiles are instrumental; a 2-ps up limit reflects the rapid thermalization, capturing, and initial cooling. (ii) The shape of the rise part of luminescence profile at 780 nm is similar to that at 770 nm, but delayed by ~ 3 ps. This implies that the emission at 780 nm does not originate from the same band as the emission at 770 nm; otherwise, the rise part of the luminescence at 780 nm should start at the same zero point as that at 770 nm. The delay of ~ 3 ps is consistent with our assignment of the emission band center

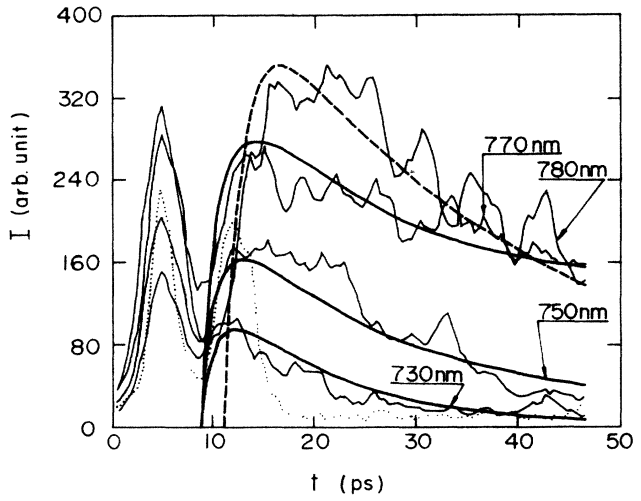

FIG. 4. Time-resolved PL profiles (thin solid curves) from the MQW at 4 K at various wavelengths. The narrow peaks within 0–10 ps are the prepulses used for averaging. The next peak of the dotted curve is the Rayleigh-scattering light from the sample surface. The thick dashed curve is generated by an expression of $I(E,t)=I_0(1-e^{-t/\tau_r})e^{-t/\tau_d}$ and the thick solid curves are generated by Eq. (1).

at 780 nm to the stimulated phonon replica. This 3 ps is the time required to establish a large population of NE phonons at q_e. (iii) The luminescence decay time[20] of 30 ps (dashed curve) for the phonon-replica emission at 780 nm is shorter than the luminescence decay time of 60 ps at 770 nm. This supports the idea that the emission at 780 nm cannot be due to impurity emission at high excitation.

To study the NE-phonon effect on energy-relaxation processes quantitatively, carrier temperature and density as function of time should be determined simultaneously. An expression in the time domain is introduced to fit the time-resolved PL data by using two adjustable parameters, namely, the carrier density[21] (n_e) and the electron temperature (T_c). For the direct optical transition in a MQW, the luminescence intensity is given by

$$I(E_i,t)=C_i(1-e^{-t/\tau_r})(|M_{e\text{-HH}}|^2\rho_e f_e \rho_{\text{HH}} f_h + |M_{e\text{-LH}}|^2\rho_e f_e \rho_{\text{LH}} f_h), \quad (1)$$

where the $\rho_{e,\text{HH,LH}}\sim m_{e,\text{HH,LH}}$ are the densities of states for the electron, heavy hole, and light hole, $M_{e\text{-HH (LH)}}$ is the matrix element[22] for the electron-to-HH (-LH) transition, C_i absorbed all the constant factors including the corrections for detector response and the transmission of each narrow-band filter used, τ_r is the rise time of luminescence and is set to be ~ 1 ps, which is an up limit of the thermalization time of the electron-hole system, and

$$f_{e,h}=\frac{1}{e^{(\varepsilon_i-u_{e,h})/k_B T_c}+1} \quad (2)$$

is the Fermi-Dirac distribution for the electrons in conduction band (with subscript e) and for the holes in the valence band (with subscript h).

A *unique* set of parameters $T_c(t)$ and $u_e(t)$ was determined by consistently fitting *all* the luminescence profiles detected at different photon energies E_i. Three calculated luminescence profiles corresponding to the experimental data are shown in Fig. 4 by the thick solid curves.

The T_c determined as a function of time is plotted as the solid curve in Fig. 5. The shaded area reflects the extent of the uncertainty in deducing the carrier temperature within the first 4 ps due to our limited time resolution. The data plotted in Fig. 5 are interpreted as follows. Carrier-carrier collisions quickly lead to a thermalized distribution at very high T_c within 1 ps due to the large number of hot carriers that are excited.[23] Although an initial thermalization process of carriers can only be probed by femtosecond spectroscopy, *an initial cooling of the thermalized distribution is studied with our present time resolution of 2 ps, providing information about the energy relaxation and the density decay of photogenerated carriers.* The initial cooling within the first 5 ps is very fast (250 K/ps), reflecting that both the screening[1] and NE-phonon effects are small. After the initial cooling, a large number of longitudinal-optical phonons in a finite wave-vector space accumulates due to the finite phonon lifetime.[24] The phonons emitted by the hot electrons are reabsorbed by the electrons as a reverse process of the emission giving rise to slower cooling for the hot carriers.[3] It should be emphasized here that the rapid initial cooling rules out the importance of significant screening of electron-phonon interaction in the present study. If the initial screening was important,[1] the initial rapid cooling would be slowed and a NE-phonon population would not be built up.

Another important observation displayed in Fig. 5 is that the time constant for the slow-decay component of the carrier-temperature cooling curve is ~ 30 ps, which is the same as the decay time of the NE-phonon–stimulated

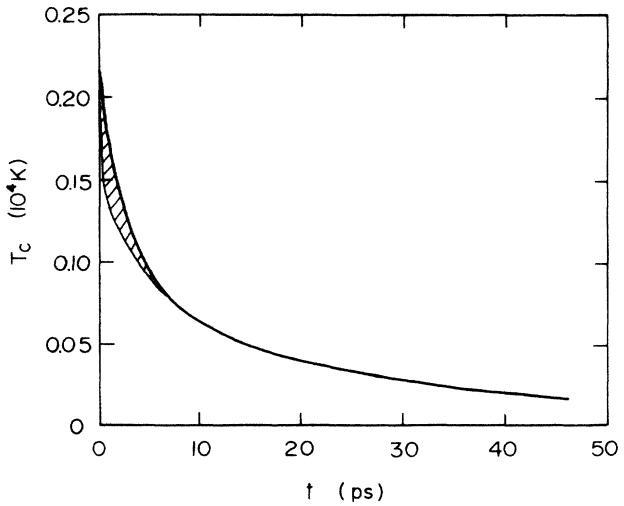

FIG. 5. Experimentally determined carrier temperature as a function of time. The shaded area indicates the extent of uncertainty in deducing carrier temperature within the first 4 ps.

phonon-replica emission at 780 nm (see Fig. 4). This suggests that ~5 ps is required for the electron system and the NE-phonon system to be essentially equilibrated with each other. The coupled electron-phonon system decays with a common decay constant of about 30 ps. It should be emphasized that this time constant (30 ps) is the lifetime of NE phonons which differ from the equilibrium phonon lifetime of ~7 ps. The lifetime for the NE phonons, longer than the equilibrium phonon lifetime, is due to the coupling between the hot electrons and NE phonons.

The determined quasi-Fermi-energies for electrons and holes are plotted in Fig. 6. The changes of u_e and u_h are very rapid, with the first 10 ps reflecting a rapid decrease of the carrier density. The behavior of the degeneracy for electrons and holes as a function of time is reversed due to the difference in effective masses for the electrons and holes.

The quasiequilibrium distribution functions for the electrons and the holes can be experimentally determined from $T_c(t)$ and $u_{e,h}(t)$. Using these distributions the energy-loss rates for the electrons and holes can be obtained. The energy-loss rate ($P_{e,\mathrm{HH}}$) is *defined* as follows:

$$P_{e,\mathrm{HH}} \equiv \frac{d\langle E\rangle_{e,\mathrm{HH}}}{dt} = \frac{d}{dt}\left[\frac{\int_0^\infty \varepsilon f(T_c,u_{e,\mathrm{HH}},\varepsilon)d\varepsilon}{\int_0^\infty f(T_c,u_{e,\mathrm{HH}},\varepsilon)d\varepsilon}\right] . \quad (3)$$

When the electron-hole system is treated as the Maxwell-Boltzmann gas, the energy-loss rate for the carriers (c =e,HH) is given by

$$P_c = k_B \frac{dT_c(t)}{dt} . \quad (4)$$

It should be pointed out that the energy-loss rates for the electrons and heavy holes obtained by Eq. (3) are the *net* loss rates. These include the energy loss due to electron (hole) -phonon interactions and the energy exchange between electrons and holes by carrier-carrier scattering. The hole-phonon scattering rate was calculated[25] and measured[6] to be 2.5–3 times larger than the rate for the electrons due to the additional coupling through the deformation potential. The energy transfer from electrons to holes should be expected in our photogenerated carrier system as long as the characteristic time for the electron-hole scattering is shorter than the electron-phonon scattering time.

The energy-loss rates determined using Eqs. (3) or (4) are shown in Fig. 7. The solid and dotted curves were obtained from Eq. (3) for the electrons and heavy holes, respectively. The dotted-dashed curve was obtained from Eq. (4). It should be pointed out that the curves obtained from either Eq. (3) or (4) are the experimental data because the distribution function $f(T_c,u_{e,h})$ was experimentally determined. The dashed line in Fig. 7 is calculated based on the simple theory[5] in which the lattice is treated as a heat bath for the quasiequilibrium carriers.

The salient features of the data displayed in Fig. 7 are as follows.

(i) The energy-loss rate for the electrons is more than 2 orders of magnitude smaller than predicted by the simple theory[5] (dashed line). The reason for the difference arises from the reheating of electrons by the NE phonons. The energy-loss rate determined for the electrons by scattering with LO phonons via the wave-vector-dependent Fröhlich interaction may be even smaller than what we have determined because the net energy-loss rate determined from Eq. (3) is the sum of rates due to electron-phonon interactions and electron-hole interactions. That P_{HH} is smaller than P_e is due to the presence of a light-

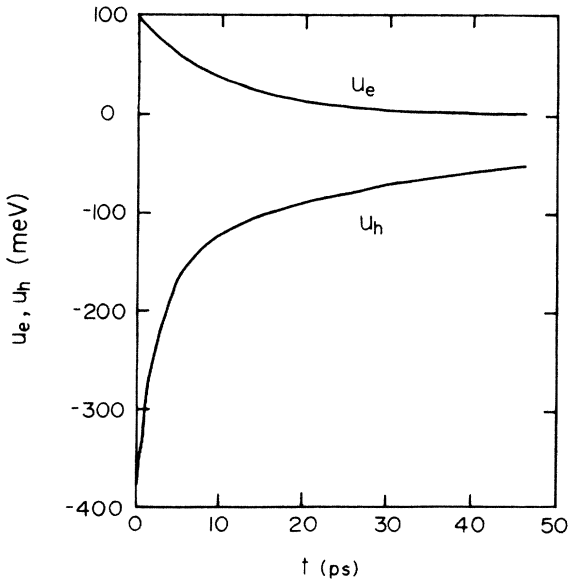

FIG. 6. Experimentally determined quasi-Fermi-energies for electrons (upper solid curve) and for holes (lower solid curve).

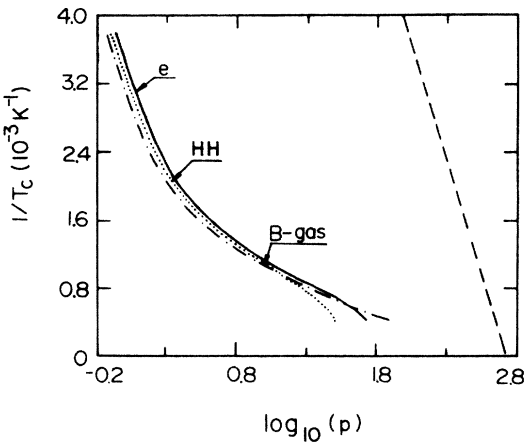

FIG. 7. Experimentally determined *net* energy-loss rates for electrons (e) and heavy holes (HH) obtained from two quasiequilibrium Fermi-Dirac distribution functions. The dotted-dashed curve is obtained from the Maxwell-Boltzmann distribution function. The dashed line is the theoretical result for bulk GaAs without the effects of screening and nonequilibrium phonons. The power unit is 10^{-10} W.

hole population and the different masses for the electrons and HH's, which leads to different behavior of quasi-Fermi-energies for the electron and HH's as a function of time.

(ii) The *net* energy-loss rates for the electrons and heavy holes almost follow the rate determined from Eq. (4). The reasons for this are the rapid decrease of u_e as shown in Fig. 6, as well as the slow cooling of the carrier temperature, which results in $u_e/k_B T_c < 0.5$, making the electron-hole system behave more like a Boltzmann gas.

(iii) The energy-loss rates increase as T_c increases. The curves in Fig. 7 even bend over and approach the maximum value of 5.3×10^{-8} W for bulk GaAs. This "bending" behavior reflects the initial rapid cooling of hot carriers and was also observed by Shah *et al.*[6] This may be the indication of the presence of NE phonons in the system.

The average phonon-emission time[7,8] for a hot carrier to emit a LO phonon is defined by

$$\tau_{\rm av}=\frac{E_{\rm LO}}{P_e}e^{-E_{\rm LO}/k_B T_c} . \tag{5}$$

The value of $\tau_{\rm av}$ as a function of the carrier temperature is plotted in Fig. 8. This is just another way to describe the energy-relaxation process. As can be seen, $\tau_{\rm av}$ *is not a constant, but is carrier-temperature dependent and, hence, time dependent.* For $T_c > 1200$ K or $t < 5$ ps, $\tau_{\rm av}$ remains at a value of about 1 ps. At the initial stage of carrier cooling, only an up limit of 0.9 ps was determined from the data shown in Fig. 4. The theoretical predicted value should be ~ 0.16 ps,[7] which is consistent with our value within the limited time resolution. As the time $t > 5$ ps (or $T_c < 1200$ K), $\tau_{\rm av}$ increases quickly with the decrease of carrier temperature, reflecting that a large NE-phonon population is built up and the carrier cooling is suppressed. At $T_c = 480$ K, $\tau_{\rm av}$ is 10 ps. Ryan *et al.*[8] obtained a constant value of 7 ps for $\tau_{\rm av}$ by studying time-resolved PL of modulation-doped MQW's. The reason for this is simply because their time resolution of ~ 20 ps did not allow them to monitor the entire carrier-cooling process.

Information about the time dependence of the initial carrier population can be obtained using the experimentally determined distribution function $f_{e,h}$. The carrier densities are obtained by the following expressions:

$$n_e(t)=\int_0^\infty \rho_e f_e \, d\varepsilon , \tag{6}$$

$$n_{\rm HH}(t)=\int_0^\infty \rho_{\rm HH} f_h \, d\varepsilon , \tag{7}$$

$$n_{\rm LH}(t)=\int_{\Delta E}^\infty \rho_{\rm LH} f_h \, d\varepsilon , \tag{8}$$

where ΔE is the energy separation between the HH and LH subbands at the zone center. The carrier densities for the electrons, heavy holes, and light holes as a function of time are plotted in Fig. 9. The quantity of $\ln[n_e(t)]$ is also plotted in this figure as a dashed curve.

The salient feature of the data in Fig. 9 is that the carrier density decreases nonexponentially and varies (by a factor of 10) rapidly within the first 30 ps after excitation by laser pulse. One cannot define a single carrier lifetime because of the nonexponential nature of the density curves. However, an effective carrier-depletion time [density decreases by a factor of e^{-1} from $n_e(t=0)$] is deduced to be as short as 10 ps. The slow component of the density-decay curve reflects part of the bimolecular recombination process. The fast decrease of carrier density occurring in such a short time period cannot be accounted for by the usual bimolecular recombination, which is a much slower process, on a nanosecond time scale in bulk GaAs and about 350 ps in a quantum-well structure with a well thickness of ~ 5 nm.[26] Several other possibilities should be pointed out and discussed.

(i) Rapid carrier-diffusion processes may be utilized[27] to shorten the lifetime of the carriers within an excited spot. Assuming that the velocity of photoexcited carriers moving in the directions perpendicular to the z axis is on an order of 10^7 cm/s, an extremely small radius of about

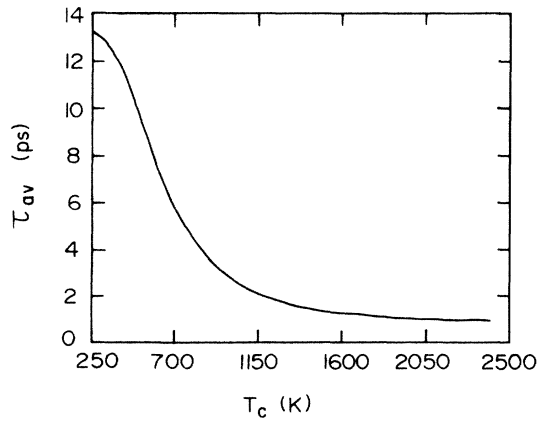

FIG. 8. Experimentally determined average phonon-emission time as a function of carrier temperature.

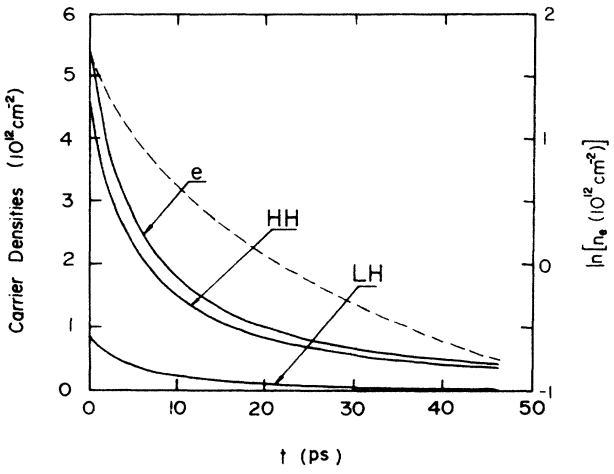

FIG. 9. Experimentally determined carrier densities as a function of time. *e* is for electron, HH for heavy hole, and LH for light hole. The dashed curve is the natural logarithmic plot of the electron density.

1 μm for the excitation spot would be required to decrease the carrier density by a factor of 10 in the excited region. Since the radius of the excitation spot was about 160 μm in our experiment, the carrier diffusion out of the excited region cannot result in the ultrafast depletion time of 10 ps.

(ii) Auger recombination resulting from strong electron-electron Coulomb interaction may be very efficient, and causes a substantial shortening of carrier lifetime at high carrier density in a quasi-two-dimensional carrier system. But from a comparative study,[28] Auger recombination in a semiconductor MQW structure and bulk were found to be close to each other. Using a value of 1.5×10^{-29} cm^6/s for the nonradiative Auger rate in bulk GaAs at room temperature,[29] the Auger-recombination lifetime at a carrier density of 10^{19} cm^{-3} should be 670 ps, which is about 100 times larger than the carrier-depletion time. However, a detailed study of Auger recombination in semiconductor MQW structures under the conditions of high carrier density, high carrier temperature, and low lattice temperature, and in the presence of a large population of NE LO phonons does not exist in the literature.

(iii) Finally, let us consider what role the NE phonons can play in reducing the initial carrier depletion time to 10 ps. As discussed in subsection A, there is a stimulated-phonon–emission process accompanied by an intense stimulated-phonon replica which is mainly radiated at the sample edge and propagates parallel to the well plane. We found that the stimulated-phonon replica detected along the y direction also had a decay time constant of about 30 ps, which is the same as that detected along the z direction. Therefore, it is most likely that the initial rapid carrier depletion is due to the participation of the NE LO phonons, which stimulates the emission of the phonon replica. It should be noted that this stimulated process is remarkably different from the regular stimulated-emission process in which phonons do not participate. As in semiconductor lasers, the stimulated emission is less effective at room temperature. Moreover, a LO-phonon replica plays no significant role in the laser operation of bulk GaAs, which is expected because of the weak electron-phonon coupling. Therefore, the prominence of phonon-assisted recombination in our quantum-well structure is due to the presence of a large number of NE LO phonons produced in the relaxation process of hot carriers. *By employing the NE-phonon model, we are able to explain not only the slow carrier cooling, but also the ultrashort carrier-depletion time in highly photoexcited undoped quantum-well structures.*

V. CONCLUSION

With 2-ps time resolution we are able to study the initial energy relaxation of the hot carriers and the decrease of carrier density simultaneously. The existence of a large population of NE phonons in highly excited semiconductor quantum-well structures is experimentally verified. Its effect on the energy relaxation is to slow down the cooling rate after an initial rapid cooling (0–5 ps). A new mechanism used to explain the ultrashort carrier-depletion time of $\sim$10 ps deduced from the fitting of time-resolved PL profiles at different emitted photon energies is proposed to be associated with NE-phonon–stimulated phonon-replica emission rather than with other nonradiative processes.

ACKNOWLEDGMENTS

The research was funded by the U.S. Air Force Office of Scientific Research under Grant No. AFOSR-86-0031. We thank Jimmy Zheng for the technical help and K. Bajaj for helpful discussions.

[1]R. J. Seymour, M. J. Junnarkar, and R. R. Alfano, Solid State Commun. **41**, 657 (1982).
[2]J. Shah, Solid-State Electron. **21**, 43 (1978).
[3]H. M. van Driel, Phys. Rev. B **19**, 5928 (1979).
[4]C. V. Shank, R. L. Fork, R. Yen, J. Shah, B. I. Greene, A. C. Gossard, and C. Weisbuch, *Solid State Commun.* **47**, 981 (1983).
[5]E. M. Conwell, *High Field Transport in Semiconductors* (Academic, New York, 1967).
[6]J. Shah, A. Pinczuk, A. C. Gossard, and W. Wiegmann, Phys. Rev. Lett. **54**, 2045 (1985).
[7]C. H. Yang, Jean M. Carlson-Swindle, A. Lyon, and J. M. Worlock, Phys. Rev. Lett. **55**, 2359 (1985).
[8]J. F. Ryan, R. A. Taylor, A. J. Turberfield, A. Maciel, J. M. Worlock, A. C. Gossard, and W. Wiegmann, Phys. Rev. Lett. **53**, 1841 (1984).
[9]K. Leo and W. W. Ruhle, Solid State Commun. **62**, 659 (1987).
[10]Kai Shum, M. R. Junnarkar, H. S. Chao, and R. R. Alfano (unpublished).
[11]R. Sooryakumar, D. S. Chemla, A. Pinczuk, A. C. Gossard, W. Wiegmann, and L. J. Sham, Solid State Commun. **54**, 859 (1985).
[12]J. E. Zucker, A. Pinczuk, D. S. Chemla, A. C. Gossard, and W. Wiegmann, Phys. Rev. Lett. **53**, 1280 (1984).
[13]H. Iwamnra, T. Saku, H. Kobayashi, and Y. Horikoshi, J. Appl. Phys. **54**, 2692 (1983).
[14]W. Cai, M. C. Marchetti, and M. Lax, Phys. Rev. B **35**, 1369 (1987).
[15]P. Lugli and S. M. Goodnick, Phys. Rev. Lett. **59**, 716 (1987).
[16]N. Holonyak, Jr., R. M. Kolbas, W. D. Laidig, B. A. Vojak, H. Hess, R. D. Dupuis, and P. D. Dapkus, J. Appl. Phys. **51**, 1328 (1980).
[17]P. Blood, E. D. Fletcher, P. J. Hulyer, and P. M. Smowton, Appl. Phys. Lett. **17**, 1111 (1986).
[18]M. S. Skolnick, K. J. Nash, P. R. Tapster, D. J. Mowbray, S. J. Bass, and A. D. Pitt, Phys. Rev. B **35**, 5925 (1987).
[19]The absolute intensity at different transition energies was obtained under the same excitation conditions. To do this, we fixed the channel-plate gain, temporal analyzer gain, and prepulse intensity, as well as the time scale for the weakest signal (at the high-energy tail) to be detected. The intensity of the prepulse was then treated as the standard of excitation level.
[20]The decay times were obtained by fitting the data in Fig. 4 to

the expression of $I(E,t)=I_0(1-e^{-t/\tau_r})e^{-t/\tau_d}$, where the parameters I_0, τ_r, and τ_d are the proportional constant, the rise time, and the decay time, respectively.

[21]The quasi-Fermi-energy of holes (u_h) is related to the quasi-Fermi-energy of electrons (u_e) and the carrier temperature by the relation $n_e=n_{\mathrm{HH}}+n_{\mathrm{LH}}$, and is given by $u_h=k_BT\ln\{\exp[a\ln(1+e^{u_e/k_BT_c})-1]\}$, where $a=m_e/(m_{\mathrm{HH}}+m_{\mathrm{LH}})$.

[22]The ratio of squared matrix elements between e-HH and e-LH was estimated from a calculation by Y. C. Chang and G. Sanders, Phys. Rev. B **32**, 5521 (1985).

[23]For a recent review, see J. Shah and R. F. Lehery, in *Semiconductors Probed by Ultrafast Laser Spectroscopy,* edited by R. R. Alfano (Academic, New York, 1984), p. 45.

[24]R. K. Chang, J. M. Ralston, and D. E. Keating, in *Proceedings of the International Conference on Light Scattering Spectra in Solids,* edited by G. B. Wright (Springer-Verlag, New York, 1969), p. 369.

[25]M. Costato and L. Reggiani, Phys. Status Solidi B **58**, 47 (1973).

[26]E. O. Gobel, H. Jung, J. Kuhl, and K. Ploog, Phys. Rev. Lett. **51**, 1588 (1983).

[27]Y. Silberger, P. W. Smith, D. J. Eilenberger, D. A. B. Miller, A. C. Gossard, and W. Wiegmann, Opt. Lett. **9**, 507 (1984).

[28]B. Sermage, D. S. Chemla, D. Sivco, and A. Y. Cho, IEEE J. Quantum Electron. **QE-22**, 774 (1986).

[29]A. Haug, J. Phys. C **16**, 4159 (1983).